

Aging of stallion spermatozoa stored in vitro is delayed at 22°C using a 67 mM glucose–10 mM pyruvate-based media

Laura Becerro-Rey¹ | Francisco Eduardo Martín-Cano¹ | Cristina Ortega Ferrusola¹ | Heriberto Rodríguez-Martínez² | Gemma Gaitskell-Phillips¹ | Eva da Silva-Álvarez¹ | Antonio Silva-Rodríguez³ | María Cruz Gil¹ | Fernando J. Peña¹ 

¹Laboratory of Equine Reproduction and Equine Spermatology, Veterinary Teaching Hospital, Universidad de Extremadura, Cáceres, Spain

²Department of Biomedical and Clinical Sciences (BKV), Obstetrics & Gynaecology (BKH), University of Linköping, Linköping, Sweden

³Facility of Innovation and Analysis in Animal Source Foodstuffs, Universidad de Extremadura, Cáceres, Spain

Correspondence

Fernando J. Peña, Laboratory of Equine Spermatology and Reproduction, Faculty of Veterinary Medicine University of Extremadura, Veterinary Teaching Hospital, Av. de la Universidad s/n, 10003 Cáceres, Spain.
Email: fjuanpega@unex.es

Funding information

Ministerio de Ciencia-European Fund for Regional Development (EFRD), Madrid, Spain, Grant/Award Number: PID2021-122351OB-I00; Junta de Extremadura-FEDER, Grant/Award Number: IB 20008; Research Council FORMAS, Grant/Award Number: 2019-00288; Ministry of Science, Madrid, Spain, Grant/Award Number: PRE2022-103090

Abstract

Background: Most commerce of equine seminal doses is carried out using commercial extenders under refrigeration at 5°C.

Objectives: To determine if 10 mM pyruvate in a 67 mM glucose extender and storage at 22°C could be the basis of an alternative storage method to cooling to 5°C.

Material and methods: Stallion ejaculates were extended in: INRA96 (67 mM glucose, non-pyruvate control), modified Tyrode's (67 mM glucose–10 mM pyruvate), supplemented with 0, 10, 50, and 100 μ M itaconate. As itaconate was vehiculated in DMSO, a control vehicle was also included. Sperm motility, viability, mitochondrial membrane potential, and production of reactive oxygen species were measured after collection and again after 48 and 96 h of storage at 22°C. To disclose molecular metabolic changes, spermatozoa were incubated up to 3 h in modified Tyrode's 67 mM glucose–10 mM pyruvate and modified Tyrode's 67 mM glucose, and metabolic analysis conducted.

Results: After 96 h of storage aliquots stored in the control, INRA96 had a very poor total motility of $5.6\% \pm 2.3\%$, while in the 67 mM glucose–10 mM pyruvate/10 μ M itaconate extender, total motility was $34.7\% \pm 3.8\%$ ($p = 0.0066$). After 96 h, viability was better in most pyruvate-based media, and the mitochondrial membrane potential in spermatozoa extended in INRA96 was relatively lower ($p < 0.0001$). Metabolomics revealed that in the spermatozoa incubated in the high pyruvate media, there was an increase in the relative amounts of NAD^+ , pyruvate, lactate, and ATP.

Discussion and conclusions: Aliquots stored in a 67 mM glucose–10 mM pyruvate-based medium supplemented with 10 μ M itaconate, maintained a 35% total motility after 96 h of storage at 22°C, which is considered the minimum acceptable motility for commercialization. Improvements may be related to the conversion of pyruvate to lactate and regeneration of NAD^+ .

This is an open access article under the terms of the [Creative Commons Attribution](https://creativecommons.org/licenses/by/4.0/) License, which permits use, distribution and reproduction in any medium, provided the original work is properly cited.

© 2023 The Authors. *Andrology* published by Wiley Periodicals LLC on behalf of American Society of Andrology and European Academy of Andrology.

KEYWORDS

artificial insemination, equine, extender, pyruvate, spermatozoa

1 | INTRODUCTION

The use of cooled semen still constitutes the core of most assisted reproductive technologies (ARTs) for equine breeding.¹ This ART was developed in the second half of the last century and established the basis of currently used commercial extenders, which saw several improvements by the end of the century. When using these extenders, refrigeration is apparently required, a handicap when considering long-haul transport of the semen, but alternatives, such as use of room-temperature storage are scarce.² The goal of refrigeration is to slow or limit sperm metabolism, to avoid the production of toxic subproducts and thus expand the lifespan of the spermatozoa while preventing the reduction of ATP content. A second objective of cooling semen is to control microbial growth in semen doses. Most commercial extenders are based on the combination of skim milk and high concentrations of glucose, which were used in the original Kenney extender.³ More recently, modifications to this basic extender occurred, mainly consisting of the incorporation of balanced salt solutions, HEPES, different combinations of antibiotics, and specific milk components like phosphocaseinates and caseins.^{1,4–7} Despite these changes in formulated combinations, most commercial extenders are still based on high concentrations of glucose. The high glucose concentrations currently found in commercial extenders are paradoxical to current knowledge on stallion sperm metabolism, a species in which oxidative phosphorylation is the main source of ATP.^{8–11} Moreover, the toxicity of high glucose concentrations to stallion spermatozoa has recently been characterized.¹² Excess glucose may generate toxic 2-oxoaldehydes, glyoxal, and methylglyoxal, which may impair sperm function. Moreover, excess glucose predisposes spermatozoa to different forms of cell death.¹³ During glycolysis for each mole of glucose, the enzyme glyceraldehyde 3 phosphate dehydrogenase (PHGDH) reduces two moles of NAD⁺ to NADH, where NADH is thereafter recycled in the mitochondria back to NAD⁺.¹⁴ Under some circumstances, however, respiration in mitochondria may not be sufficient to recycle enough NAD⁺ for efficient glycolysis, and alternative mechanisms ought to be present to regenerate NAD⁺ through the lactate dehydrogenase (LDH) enzyme, reducing pyruvate to lactate. This aerobic glycolysis reaction occurs under high oxygen concentrations and is termed the Warburg effect.¹⁵

These recent developments on our understanding of stallion sperm metabolism may constitute a basis for development of alternative extenders, which may permit modification of sperm metabolism and the conservation of stallion spermatozoa for longer periods at temperatures around 20°C. Moreover, the use of minimal contamination protocols during semen preparation may also reduce bacterial contamination in commercial doses.

Most commercial extenders contain high concentrations of glucose, but lack pyruvate in their composition. While glucose at physiological concentrations is essential for sperm function,^{16–21} the interaction

of glucose with other components in the media may be even more important than glucose concentration per se.¹⁸ For instance, a supply of pyruvate converted to lactate may improve glycolysis efficiency and could be used as a strategy to improve the metabolic efficiency of the spermatozoa under high glucose concentrations.²² Itaconate, considered a regulator of cellular metabolic reprogramming, is generated by the conversion of cis-aconitate, an intermediate of the Krebs cycle, and may play a role in diverting glucose metabolism from glycolysis to the pentose phosphate pathway, contributing to the regulation of redox homeostasis.²³ Addition of itaconate to boar spermatozoa in a high 30 mM glucose media, improved sperm motility.²⁴

In this study, we followed the hypothesis that an increased concentration of pyruvate in a media with high concentration of glucose may improve preservation of stallion spermatozoa at room temperature, a major advantage if refrigeration can be avoided. In addition, the potential beneficial effect of itaconate was also investigated.

2 | MATERIALS AND METHODS

2.1 | Reagents and media

Chemicals were purchased from Sigma Aldrich. All other reagents for flow cytometry were purchased from Thermofisher. ViaKrome 808 Fixable Viability Dye was purchased from Beckman Coulter. Ultra-pure deionized water (>18.2 MΩ cm) was produced from a Elga Purelab Quest U.V. (www.elgalabwater.com).

2.2 | Semen collection and processing

Semen was collected from four fertile stallions housed according to institutional and European animal care regulations (Law 6/2913 June 11th and European Directive 2010/63/EU). Routine semen collection from stallions that are used for commercial semen production did not require ethical approval. Ejaculates were collected using a pre-warmed, lubricated Missouri model artificial vagina following standard veterinary practices. After collection, the ejaculate was immediately evaluated for sperm motility and concentration and processed in the adjacent laboratory. Colloidal centrifugation²⁵ was performed to remove dead spermatozoa and contaminating particles from the ejaculate. The pellet was re-extended to a final concentration of 25×10^6 spermatozoa/mL in 67 mM glucose–10 mM pyruvate Tyrode's media (76 mM NaCl, 3.1 mM KCl, 2 mM CaCl₂·2H₂O, 0.4 mM MgSO₄·7H₂O, 0.3 mM KH₂PO₄, 20 mM HEPES, 67 mM glucose, 21.7 mM Na lactate, 10 mM Na pyruvate, 13 mM NaHCO₃, 3 mg/mL BSA, 0.058 g/L penicillin, and 0.05 g/L dihydrostreptomycin sulfate) pH 7.4,²⁶ or a commercial extender INRA96 (IMV), formulated with 67 mM

glucose, but lacking pyruvate.²⁷ To minimize bacterial contamination, semen processing was conducted in a laminar flow cabinet.

2.3 | Experimental design

1. Experiment I: Role of a pyruvate-based extender in improving the functionality of stallion spermatozoa during incubation at 22°C for 96 h.

Stallion ejaculates were processed, split sampled, and extended in a high glucose (67 mM), high pyruvate (10 mM)-based media supplemented with 0 (control), 10, 50, and 100 μ M itaconate. Itaconate was vehiculated in DMSO, so a control vehicle for the DMSO (VEH) was also included. Extension in INRA96 was used as a non-pyruvate control. INRA96 was included as a control, as it is a well-validated, widely commercially used equine semen extender, which has a glucose concentration of 67 mM, but does not contain pyruvate. At 0, 48, and 96 h of storage at 22°C, evaluation of motility characteristics (computer-assisted sperm analysis [CASA]), viability, function, mitochondrial membrane potential, mitochondrial mass, and production of reactive oxygen species (ROS) was performed.

2. Experiment II: Identification of changes in the metabolome induced by 10 mM pyruvate in a 67 mM glucose extender.

To test the hypothesis that pyruvate improves metabolic efficiency in a high-glucose extender, aliquots of stallion spermatozoa were incubated at 37°C for up to 3 h in a high glucose (67 mM glucose) and in a 67 mM glucose–10 mM pyruvate media. CASA analysis, flow cytometry, and directed metabolomics were conducted after the end of the incubation period.

2.4 | Computer-assisted sperm analysis

Sperm motility and kinematics were assessed using a CASA system (ISAS Proiser) according to standard protocols used at our center.²⁸ Semen samples were loaded in a Leja chamber with a depth of 20 μ m (Leja), and placed on a stage warmed to 37°C. Analysis was based on evaluation of 60 consecutive digitized images captured in 1 s, with a frame rate of 60 Hz, obtained using a 10 \times negative-phase contrast objective (Olympus CX 41). ISAS v.1.2 software settings were automatically set for horses, with minor modifications herein described. At least 500 spermatozoa per sample were analyzed in random fields; the area of the particles to consider were between 4 and 75 μ m², the algorithm for advanced tail analysis was applied. Any particles incorrectly identified as spermatozoa were detected and these were discarded using the play back function. Spermatozoa curvilinear velocity (VCL) greater than 10 μ m/s and less than 45 μ m/s were considered low-speed spermatozoa, those with a VCL more than 45 μ m/s and less than 90 μ m/s were considered as medium-speed spermatozoa, and those with a VCL greater than 90 μ m/s were considered rapid spermatozoa. Spermatozoa deviating less than 45% from a straight line were classified as

linearly motile. Other parameters studied included VCL (μ m/s), defined as the timeline average velocity of a sperm head along its actual trajectory; the straight-line velocity (VSL, μ m/s), the velocity calculated along a straight line between the first and last points of the path; and velocity along the average path (VAP, μ m/s) as the time-averaged velocity calculated along the average path.

2.5 | Flow cytometry

Flow cytometry analyses were conducted using a Cytoflex S flow cytometer (Beckman Coulter) equipped with violet, blue, yellow, and red lasers, and a Cytoflex LX equipped with ultraviolet, violet, blue, yellow, red, and infrared lasers. The instruments were calibrated daily using specific calibration beads provided by the manufacturer. A compensation overlap was performed before each experiment. Files were exported as Flow Cytometry Standard (FCS) files and analyzed in Cytobank Software (Beckman Coulter). Unstained, single-stained, and fluorescence minus one (FMO) controls were used to determine compensations and positive and negative events, as well as to set regions of interest as described in previous publications by our laboratory.^{29,30}

2.6 | Five-color assessment of sperm function

A five-color panel was created to simultaneously assess a wide range of sperm components and functions, including viability, membrane permeability, mitochondrial membrane potential, mitochondrial mass, and apoptotic changes. Stallion spermatozoa were stained with Hoechst 33342 0.3 μ M (ThermoFisher; Ex/Em [nm] 365/485); 30 min at 37°C in the dark. Then YoPro-1 (ThermoFisher Y3603; 12.5 nM, Ex/Em [nm] 491/509); tetramethylrhodamine TMRM (ThermoFisher I34361; 50 nM; Ex/Em [nm] 548/574); MitoTracker Deep Red (ThermoFisher M46753; 50 nM; Ex/Em [nm] 644/665); and ViaKrome 808 (Beckman Coulter C36628 2 μ L/sample; Ex/Em [nm] 854/878) were added and samples were incubated in the dark at 37°C for 20 min; then samples were washed and resuspended in phosphate-buffered saline (PBS) and run in the flow cytometer (Cytoflex LX).

2.7 | Four-color panel display (JC-1, CellROX Deep Red, Live/Dead)

Aliquots of stallion spermatozoa were stained with JC-1 (to assess mitochondrial membrane potential; 1 μ M, Ex 561 nm, Em 590 nm aggregates and Ex 488 nm, Em 529 nm, monomers) in the dark at 37°C, 2 μ M of CellROX Deep Red (to assess the production of ROS; Ex 638 nm, Em 665 nm) and incubated for 30 min in the dark at 37°C. Then 0.5 μ L of Live/Dead violet solution (to assess sperm viability; Ex 405 nm, Em 450 nm) were added to 500 μ L of sperm suspension and incubated for 10 min in the dark at 37°C. Cells were washed twice, resuspended in PBS, and run in the flow cytometer (Cytoflex S).

2.8 | Metabolite analysis of nucleosides, nucleotides, amino acids, sugars, and organic acids by UHPLC-MS QqQ

Samples were washed twice in PBS ($600 \text{ g} \times 10^6$), then the pellet formed by the spermatozoa was frozen immediately in liquid nitrogen and kept frozen at -80°C until analysis. The sperm pellet was then re-extended in 300 mL Milli-Q water and sonicated for 3 s. Immediately afterward, it was centrifuged at $6452 \times g$ at 4°C for 3 min, and the supernatant was injected into the UHPLC-MS/MS. These metabolites were analyzed by a UHPLC/MS/MS system consisting of an Agilent 1290 Infinity II Series HPLC (Agilent Technologies) equipped with an automated multisampler module and a high-speed binary pump, coupled to an Agilent 6470 QqQ mass spectrometer (Agilent Technologies) using an Agilent Jet Stream Dual electrospray (AJS-Dual ESI) interface. The HPLC and QqQ detector were controlled using MassHunter Workstation Data Acquisition software (Agilent Technologies, Rev. B.08.00). The sample was injected onto an Agilent HILIC-Z HPLC column (4.6 mm, 100 mm, $2.1 \mu\text{m}$, Agilent Technologies), thermostated at 35°C , at a flow rate of 0.4 mL/min. The injection volume was $7 \mu\text{L}$. For gradient elution, solvent A was 10 mM ammonium acetate at a pH 9 in Milli Q water, and solvent B was 10 mM ammonium acetate at a pH 9 in Milli Q water:acetonitrile 10:90. To start with 98% solvent B was maintained until 5 min. Solvent B was then decreased from 98% to 60% from 5 to 10 min and held at 60% for an additional 2 min. Then solvent B returned to the initial conditions up to 15 min. The mass spectrometer was operated in negative mode and was run in MS/MS mode. Nitrogen was used as a nebulizing gas, drying gas, sheath gas, and collision gas. The nebulizer gas pressure was set to 35 psi, whereas the drying gas flow was set to 12 L/min at a temperature of 250°C , and the sheath gas flow was set to 15 L/min at a temperature of 350°C . The capillary spray and fragmenting voltages were 3500 and 100 V, respectively. The MRM conditions were optimized by injecting a standard solution of each metabolite at different collision energy (CE). Data processing and analysis were performed using the MassHunter Quantitative Analysis software (Rev B.07.00.201, Agilent Technologies).

2.9 | Statistical analysis

All experiments were repeated at least three times with independent biological replicates (four different stallions, three replicates each, $n = 12$). The normality of the data was assessed using the Kolmogorov–Smirnov test. One-way ANOVA followed by Dunnett's multiple comparisons test were performed using GraphPad Prism version 10.00 for Mac (www.graphpad.com). Differences were considered significant when $p < 0.05$. Results are displayed as means \pm SEM. Computational flow cytometry³¹ was conducted as follows: all replicates were concatenated to obtain a single FCS file of each condition in compensated data on the whole sperm population, after the exclusion of doublets and clumps.³² UMAP analysis was performed in CytoBank (Beckman Coulter; <https://premium.cytobank.org>).^{33–35} Analysis

of the metabolomic data was performed using QluCore Omics Explorer (<https://qlucore.com>).^{36,37}

3 | RESULTS

3.1 | Motility and velocities

No differences in motility were observed at $t = 0$ (Figure 1A). Analysis was conducted shortly after processing and extension of the spermatozoa in the different media, and within the first 2 h after collection. However, after 48 h of storage at 22°C , differences became evident. All the high-pyruvate-derived extenders used maintained high percentages of motile spermatozoa. While aliquots of stallion spermatozoa extended in the control INRA96 showed a total motility (TM) percentage (CASA) of $29.5\% \pm 5.0\%$, aliquots extended in the 67 mM glucose–10 mM pyruvate media had a TM of $64.8\% \pm 3.8\%$ (Figure 1B; $p < 0.0001$), and aliquots extended in the 67 mM glucose–10 mM pyruvate/10 μM itaconate had a TM of $68.5\% \pm 3.9\%$ (Figure 1B; $p < 0.0001$). After 96 h of storage, aliquots stored in the control INRA96 had very poor TM $5.6\% \pm 2.3\%$, while the TM of aliquots stored in the 67 mM glucose–10 mM pyruvate/10 μM itaconate extender was $34.7\% \pm 3.8\%$ (Figure 1C; $p = 0.0066$). The percentages of linear motile spermatozoa at the beginning of storage ($t = 0$) were greater in spermatozoa stored in the control INRA96 extender (Figure 1D; $p = 0.0007$, 0.0108, 0.0001, and 0.0003), but the aliquot of spermatozoa stored in the 67 mM glucose–10 mM pyruvate/100 μM itaconate had a percentage of linear motile spermatozoa comparable to the aliquot extended in control INRA96 (Figure 1D). After 48 and 96 h of incubation, the percentages of linear motile spermatozoa were much lower in the aliquots of stallion spermatozoa stored in control INRA96 than aliquots stored in the 67 mM glucose–10 mM pyruvate with either 10 and 50 μM itaconate after 48 h and with 10, 50, and 100 μM itaconate after 96 h of storage (Figure 1E,F). The sperm velocities VCL, VAP, and VSL were improved in all the variations of the extenders supplemented with itaconate with respect to the aliquots stored in control INRA96 and from the first day of incubation ($t = 0$; Figure 2). While sperm VCL at $t = 0$ in the control INRA96 was 79.0 ± 3.1 , in the 67 mM glucose–10 mM pyruvate media, it was $128.3 \pm 4.5 \mu\text{m/s}$ (Figure 2A; $p = 0.0002$). Likewise, aliquots supplemented with itaconate showed increased VCL in comparison to control INRA96. The same trend was observed after 48 and 96 h of storage (Figure 2B,C). A similar trend was observed with VSL and VAP, with greater sperm velocities displayed throughout the storage period in all pyruvate-based media in comparison with the commercial extender INRA96 (Figure 2D–I). Moreover, itaconate supplementation significantly increased these differences (Figure 2D–I).

3.2 | Viability and membrane permeability

Representative cytograms of the assay are shown in Figure 3, panel 1. After collection and processing ($t = 0$), viability was significantly

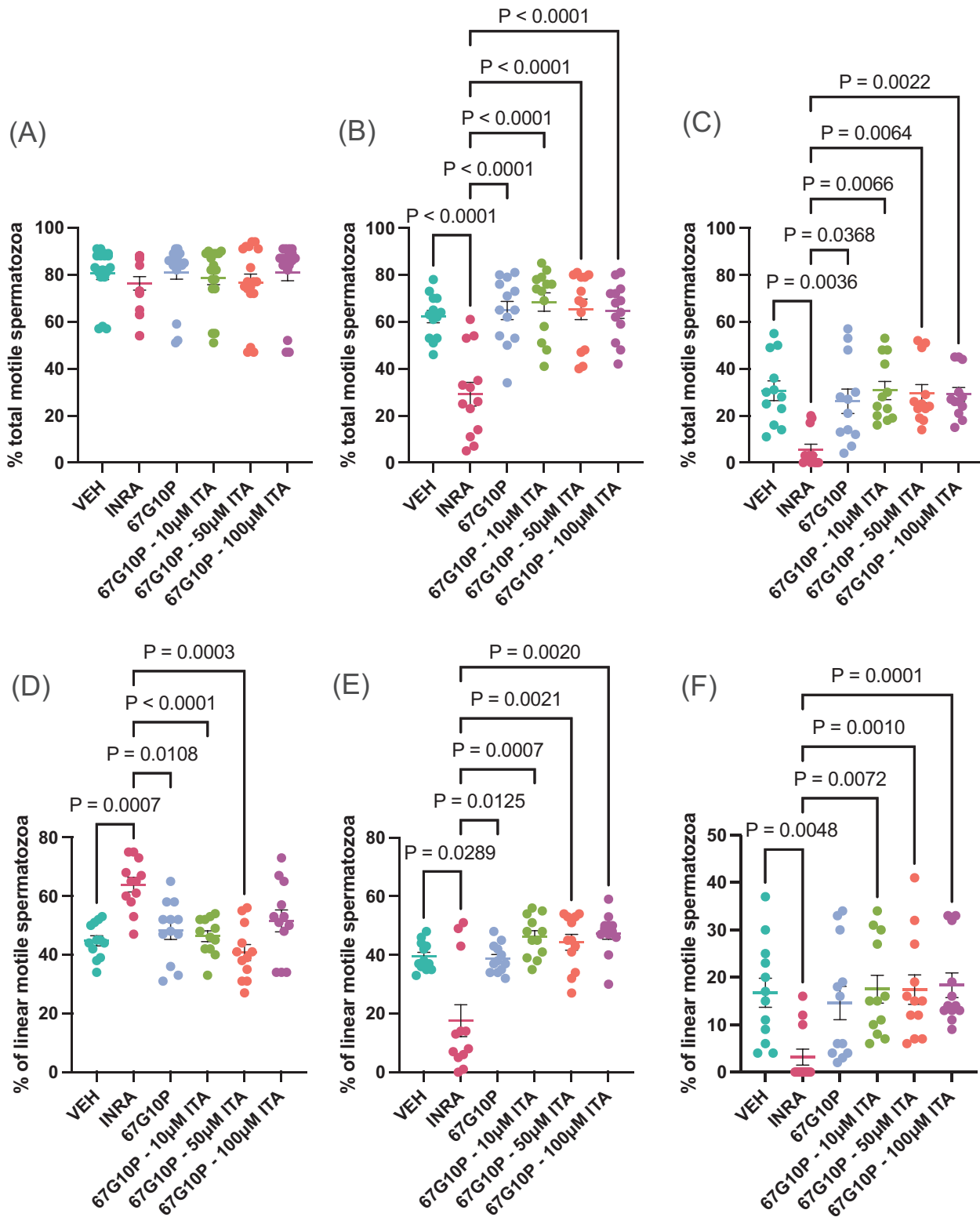


FIGURE 1 Changes in the percentages of total and linear motile stallion spermatozoa, processed as described in Materials and Methods section. Computer-assisted sperm analysis (CASA) was conducted shortly after collection and processing ($t = 0$), and after 48 and 96 h of storage at 22°C. (A) Percentage of total motile spermatozoa at $t = 0$, (B) after 48 h, and (C) after 96 h. (D) Percentage of linear motile spermatozoa on Day 1 after 3 days, and (E) after 5 days of storage at 22°C. VEH: control vehicle; INRA: spermatozoa stored in a commercial extender; 67G10P: modified Tyrode's media with 67 mM glucose and 10 mM pyruvate; 67G10P-10 μ M ITAC: modified Tyrode's media supplemented with 10 μ M itaconate; 67G10P-50 μ M ITAC: modified Tyrode's media supplemented with 50 μ M itaconate; 67G10P-100 μ M ITAC: modified Tyrode's media supplemented with 100 μ M itaconate. Data are expressed as means \pm SEM and derived from three independent ejaculates from four different stallions ($n = 12$).

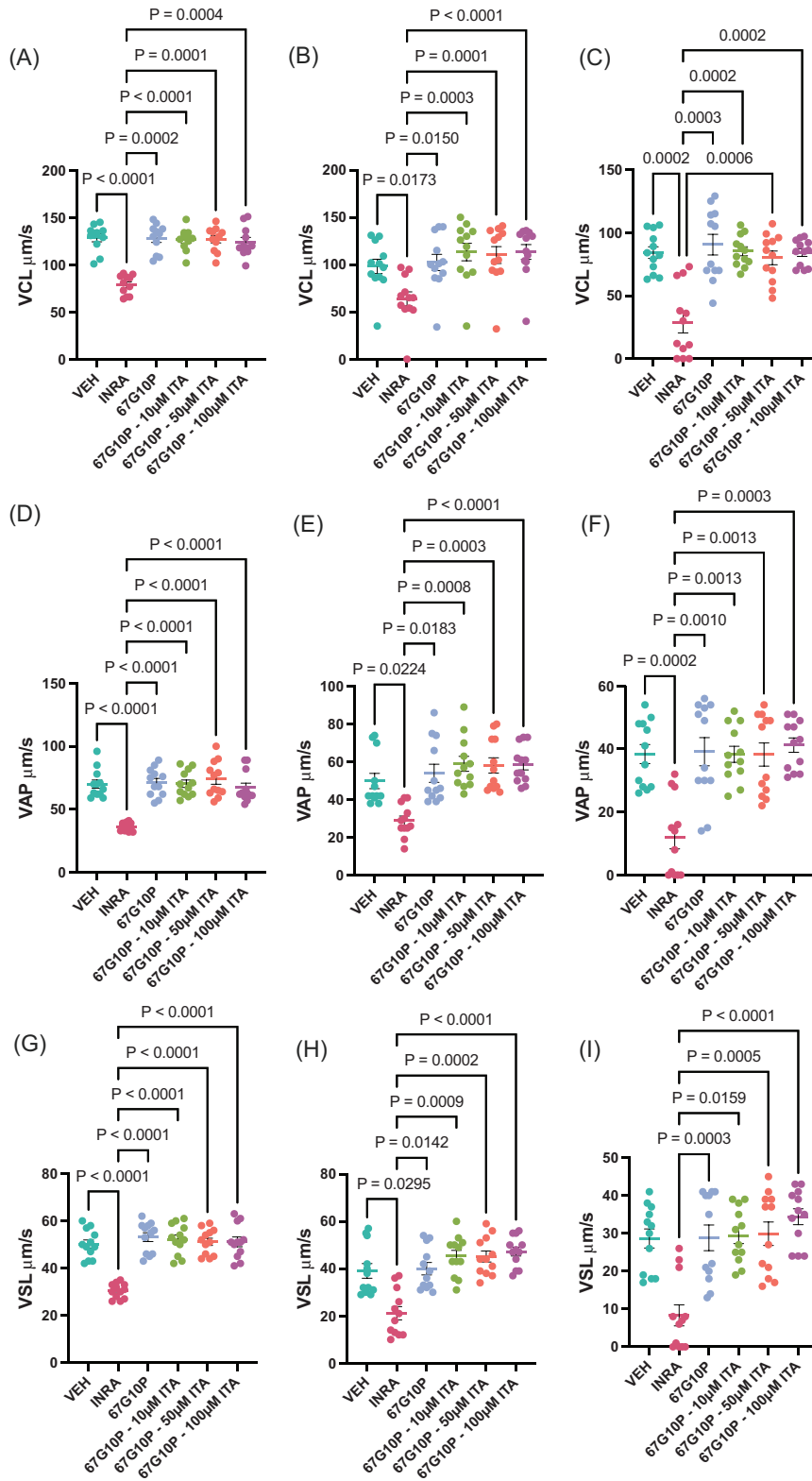


FIGURE 2 Changes in sperm velocities, VCL (circular velocity, $\mu\text{m/s}$), VAP (average path velocity, $\mu\text{m/s}$) VSL (straight line velocity, $\mu\text{m/s}$) in stallion spermatozoa stored in different media for up to 96 h. (A) VCL shortly after collection and processing and storage at 22°C, $t = 0$. (B) VCL after 48 h of storage. (C) VCL after 96 h of storage. (D–F) VAP shortly after collection and processing ($t = 0$), after 48 h, and after 96 h of storage at 22°C. (G–I) VSL shortly after collection and processing ($t = 0$), 48, and 96 h. VEH: control vehicle; INRA: spermatozoa stored in the commercial extender; 67G10P: modified Tyrode's media with 67 mM glucose and 10 mM pyruvate; 67G10P-10 μM ITAC: modified Tyrode's media supplemented with 10 μM itaconate; 67G10P-50 μM ITAC: modified Tyrode's media supplemented with 50 μM itaconate; 67G10P-100 μM ITAC: modified Tyrode's media supplemented with 100 μM itaconate. Data are expressed as means \pm SEM and derived from three independent ejaculates from four different stallions ($n = 12$).

greater in aliquots stored in the control commercial extender INRA96 (Figure 3, $p < 0.0001$), with respect to most of the variants of the experimental 67 mM glucose-10 mM pyruvate-based extender, except for the variant supplemented with 10 μM itaconate, which showed similar viability to the aliquot extended in control INRA96, and was superior to that observed in the unsupplemented 67 mM glucose-10 mM pyruvate

extender (Figure 3A). However, viability was improved after 48 h of storage in the 67 mM glucose-10 mM pyruvate extender ($53.6\% \pm 3.5\%$ vs. $61.3\% \pm 1.6\%$ in INRA96 and 67 mM glucose-10 mM pyruvate, respectively, $p = 0.0278$; Figure 3B). After 96 h of storage at room temperature, viability was better in most 67 mM glucose-10 mM pyruvate-based media variants. The viability of spermatozoa stored in control

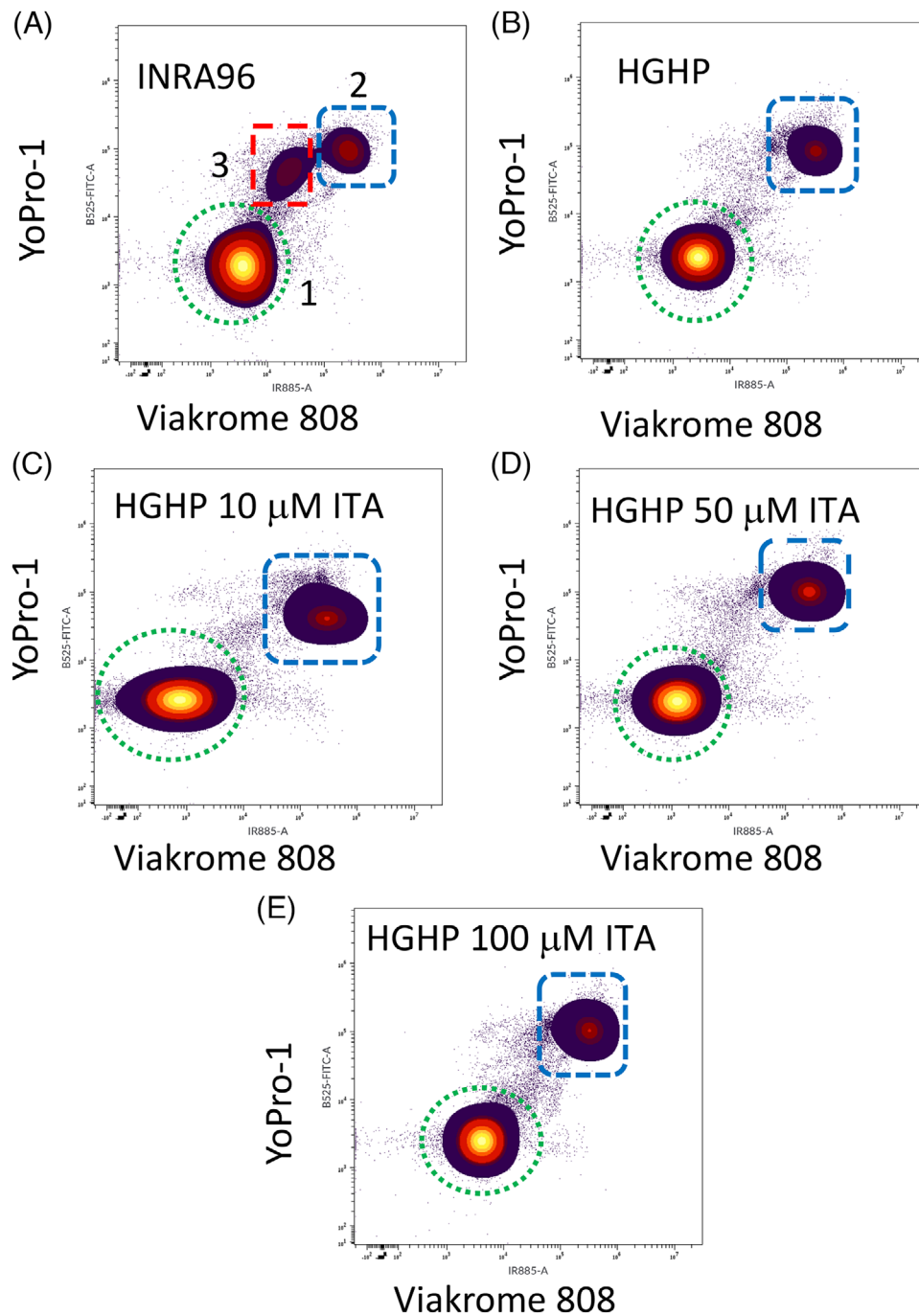


FIGURE 3 Panel 1. Representative cytograms of the flow cytometry assay, showing three distinct populations: (1) represents viable spermatozoa, negative for YoPro-1 and Viakrome 808, (3) represents live spermatozoa (Viakrome 808 negative) with increased membrane permeability (YoPro-1 positive), and population (2) represents necrotic spermatozoa, positive for both YoPro-1 and Viakrome 808. As seen in (a), the population of spermatozoa with increased membrane permeability is more evident in the aliquot of stallion spermatozoa incubated in the commercial extender, while negligible in all the aliquots of stallion spermatozoa incubated in the high-glucose high-pyruvate modified Tyrode's extenders (b–e). Panel 2. Changes in the percentages of viable spermatozoa shortly after collection and processing ($t = 0$) (A), after 48 h (B), and after 96 h (C) of storage at 22°C. (D–F) Changes in membrane permeability shortly after collection and processing ($t = 0$), and after 48 and 96 h of storage at 22°C. (G–I) Changes in the percentage of necrotic spermatozoa shortly after collection and processing ($t = 0$), and after 48 and 96 h of storage at 22°C, respectively. VEH: control vehicle; INRA: spermatozoa stored in the commercial extender; 67G10P: modified Tyrode's media with 67 mM glucose and 10 mM pyruvate; 67G10P–10 μ M ITAC: modified Tyrode's media supplemented with 10 μ M itaconate; 67G10P–50 μ M ITAC: modified Tyrode's media supplemented with 50 μ M itaconate; 67G10P–100 μ M ITAC: modified Tyrode's media supplemented with 100 μ M itaconate. Data are expressed as means \pm SEM and derived from three independent ejaculates from four different stallions ($n = 12$).

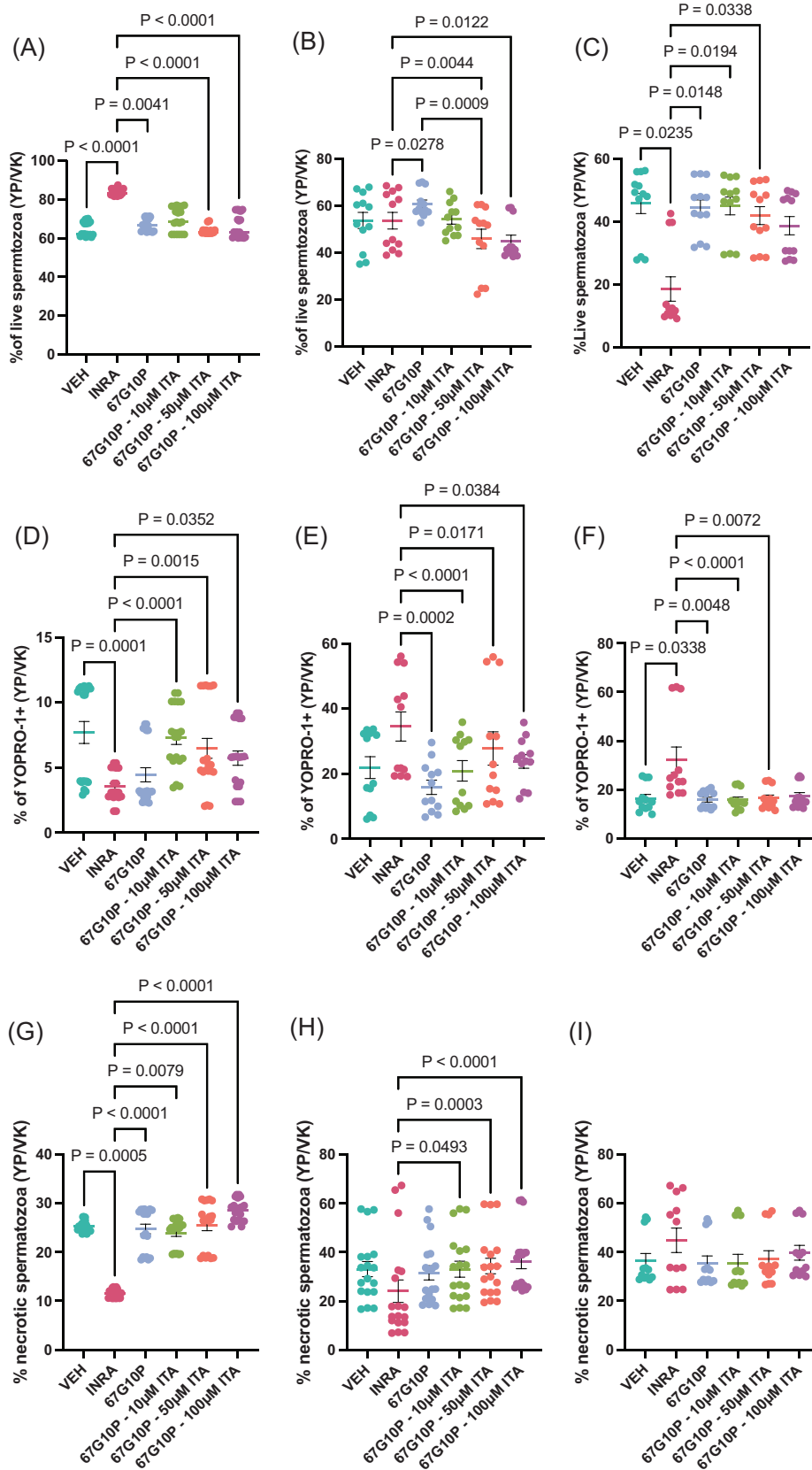


FIGURE 3 Continued

INRA96 dropped dramatically to $18.3\% \pm 3.9\%$, whereas sperm viability in the 67 mM glucose–10 mM pyruvate-derived media was over 40%, with $44.4\% \pm 2.5\%$ and $45.5\% \pm 2.8\%$ in spermatozoa stored in the 67 mM glucose–10 mM pyruvate and 67 mM glucose–10 mM pyruvate/10 μM itaconate, respectively ($p = 0.0148$ and 0.0194 ; Figure 3C). Interestingly, changes in viability were mostly because of the increased permeability to YoPro-1 in live spermatozoa (Figure 3D–F). This was particularly evident after 96 h of storage at room temperature, where spermatozoa stored in control INRA96 displayed $32.3\% \pm 5.2\%$ of YoPro-1+ (and Viakrome 808 negative), while the percentage of YoPro-1+ spermatozoa were half this value, respectively, $15.9\% \pm 1.0\%$ ($p < 0.0040$) and $15.8\% \pm 1.1\%$ while stored in the 67 mM glucose–10 mM pyruvate and 67 mM glucose–10 mM pyruvate/50 μM itaconate, ($p < 0.0001$; Figure 3F). This increase in the YoPro-1 positivity was also evident in UMAP clustering analysis (Figure S2).

3.3 | Mitochondrial membrane potential ($\Delta\Psi_m$)

Mitochondrial membrane potential was investigated in two different multicolor panels, using either TMRM or JC-1. Representative cytograms of both assays are presented in Figure 4, panel 1. At the beginning of incubation ($t = 0$), both methods revealed that the mitochondrial membrane potential was greater in spermatozoa stored in the commercial extender INRA96 (Figure 4, panel 2 A,B). When $\Delta\Psi_m$ was measured using TMRM, no differences were present between spermatozoa stored in INRA96 and those stored in the 67 mM glucose–10 mM pyruvate media, but a drop in $\Delta\Psi_m$ was observed in spermatozoa incubated in the 67 mM glucose–10 mM pyruvate media when JC-1 was used as a method for the determination of the mitochondrial membrane potential (Figure 4B; $p = 0.0059$). After 48 h of storage, the mitochondrial membrane potential was lower in spermatozoa stored in the control commercial extender INRA96 (Figure 4C,D). When TMRM was used to determine the $\Delta\Psi_m$ after 96 h of storage, this was significantly lower only with respect to spermatozoa stored in the 67 mM glucose–10 mM pyruvate/10 μM itaconate (Figure 5E; $p = 0.0007$). However, when the mitochondrial membrane potential was measured using JC-1, the mitochondrial membrane potential in spermatozoa extended in the commercial control INRA96 was significantly lower with respect to all other media (Figure 4F; $p < 0.0001$).

3.4 | Production of reactive oxygen species

Production of ROS was simultaneously measured alongside $\Delta\Psi_m$ (JC-1 staining), using CellROX Deep Red. According to the manufacturer, this probe is mainly sensitive to superoxide anion ($\text{O}_2^{\cdot-}$); however, it is also sensitive to the hydroxyl radical ($\cdot\text{OH}$). Representative cytograms of the assay are provided in Figure 5. Shortly after processing, no differences were observed in any of the groups considered with respect to ROS production; yet there was a large variability among groups (Figure 5A). After 48 h of storage, ROS production was greater in spermatozoa stored in the 67 mM glucose–10 mM pyruvate and

67 mM glucose–10 mM pyruvate/50 μM itaconate extenders compared with the control INRA96 extender (Figure 5B; $p = 0.0013$ and 0.0487). Finally, after 96 h of storage, ROS production was greater in all media compared with the control INRA96 (Figure 5C). Although the production of ROS, particularly $\text{O}_2^{\cdot-}$, has been considered a consequence of mitochondrial activity, discrepancies observed in our results, especially at $t = 0$ and after 48 h of storage, led us to use computational flow cytometry to further investigate this aspect. We used UMAP (uniform manifold approximation and projection for dimension reduction) on the Cytobank (Beckman Coulter) platform.^{34,35,38} Representative results of the UMAP analysis are presented in Figure S1. Noteworthy findings were the altered map of the samples stored in the control commercial extender INRA96. In addition, when fluorescence from each channel was investigated on the z axis, very poor JC-1 fluorescence was present, compared with spermatozoa stored in all the other media. The more remarkable finding was the presence of a population of spermatozoa producing high amounts of ROS, but, unlike in all other media, in the spermatozoa stored in control INRA96, the changes were unrelated to high mitochondrial activity (Figure S1 red dotted circle).

3.5 | Mitochondrial mass

Mitochondrial mass differed among media and time of storage. On Day 1, mitochondrial mass was significantly greater in spermatozoa stored in the control INRA96 (Figure S2), while after 48 and 96 h of storage, mitochondrial mass was significantly reduced in INRA96 control spermatozoa. Although mitochondrial mass followed a pattern similar to mitochondrial membrane potential, computational cytometry revealed that both populations were not equivalent (Figure S2). TMRN and Mitotracker deep red fluorescence was depicted in the Z channel in UMAP analysis, clearly showing that not all the mitochondria (mitochondrial mass) had high mitochondrial membrane potential (circles).

3.6 | Metabolomic profile

To disclose metabolic molecular mechanisms behind the role of pyruvate that may help to explain the improvement seen, incubation experiments were conducted in two different variants of Tyrode's media: a media with 67 mM glucose (high glucose) and with 67 mM glucose and 10 mM pyruvate (high pyruvate). After 3 h of incubation at 37°C, the metabolic profile was analyzed. The most relevant changes observed (Figure 6) were an increase in the relative amounts of *NAD⁺, fumarate, pyruvate, lactate, ribulose 5 phosphate, ATP, galactose, and urea*, in the spermatozoa incubated in the 67 mM glucose–10 mM pyruvate media. The percentage of live spermatozoa was also higher in stallion spermatozoa incubated in the 67 mM glucose–10 mM pyruvate media. To the contrary, the following metabolites were less abundant in the 67 mM glucose–10 mM pyruvate media: *NADH, dihydroxyacetone phosphate, fructose 1, 6 biphosphate* and especially *phosphoenolpyruvate*.

4 | DISCUSSION

In the present study, we investigated whether the addition of pyruvate may extend stallion sperm lifespan in a high-glucose media during storage at 22°C for 96 h, a desirable management condition avoiding refrigeration. On the first day of storage, most functional parameters were better in aliquots of spermatozoa stored in the control commercial extender (INRA96), an extender with a 67 mM glucose concentration, but which does not contain pyruvate. However, after 48 h of storage, and especially after 96 h of storage at 22°C, all the parameters of sperm functionality studied were better in pyruvate-based media. On Day 1 ($t = 0$), the high 67 mM glucose–10 mM pyruvate media

supplemented with 100 μM itaconate showed the best results, suggesting that under some circumstances, supplementation with itaconate may be positive. As the storage period advanced, the stallion spermatozoa extended in the control commercial extender INRA96 revealed a progressively more permeable membrane, an effect not seen in the spermatozoa extended in the 67 mM glucose–10 mM pyruvate-based media, in which the sperm membrane maintained integrity during all the storage period assayed. After 96 h of storage, the loss of membrane integrity was because of the increased membrane permeability, as revealed by the increase in YoPro-1 staining. Increased membrane permeability is linked to lipid peroxidation,^{39–41} a characteristic of cell aging. During the initial steps of cellular senescence, specific pannexin-

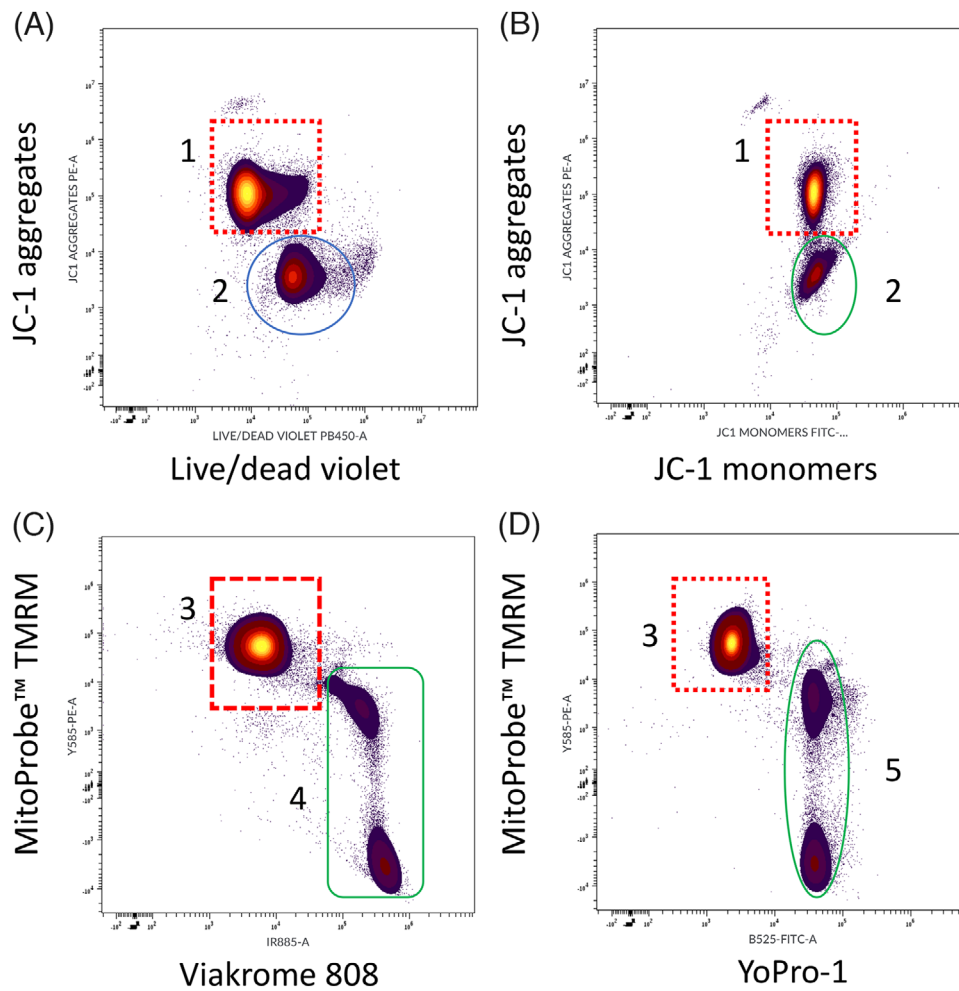


FIGURE 4 Panel 1. Representative cytograms of the flow cytometry assays for the measurement of mitochondrial membrane potential ($\Delta\Psi_m$); measured in (a) and (b), with the JC-1 probe, and in (c) and (d) with MitoProbe TMRM. (a) Double staining with Live/Dead Violet and JC-1: (1) represents live spermatozoa (Dim for live dead violet) with high $\Delta\Psi_m$, (2) are dead spermatozoa (Bright for Live/Dead violet). (b) JC-1 staining showing spermatozoa with high $\Delta\Psi_m$ (1: orange fluorescence) and low $\Delta\Psi_m$ (2: green fluorescence). (c and d) The assessment of $\Delta\Psi_m$ using MitoProbe TMRM with necrotic spermatozoa gated out in (c) after staining with Viakrome 808 (4) and with YoPro-1 (5) in (d). Spermatozoa showing $\Delta\Psi_m$ (3). Panel 2. Percentages of stallion spermatozoa showing high $\Delta\Psi_m$ measured using MitoProbe TMRM shortly after collection and processing ($t = 0$) (A) and after 48 h (C) and 96 h (E) of storage at 22°C, and measured using JC-1 shortly after collection and processing ($t = 0$) (A), after 48 h (C), and after 96 h (E) of storage at 22°C. VEH: control vehicle; INRA: spermatozoa stored in the commercial extender; 67G10P: modified Tyrode's media with 67 mM glucose and 10 mM pyruvate; 67G10P–10 μM ITAC: modified Tyrode's media supplemented with 10 μM itaconate; 67G10P–50 μM ITAC: modified Tyrode's media supplemented with 50 μM itaconate; 67G10P–100 μM ITAC: modified Tyrode's media supplemented with 100 μM itaconate. Data are expressed as means \pm SEM and derived from three independent ejaculates from four different stallions ($n = 12$).

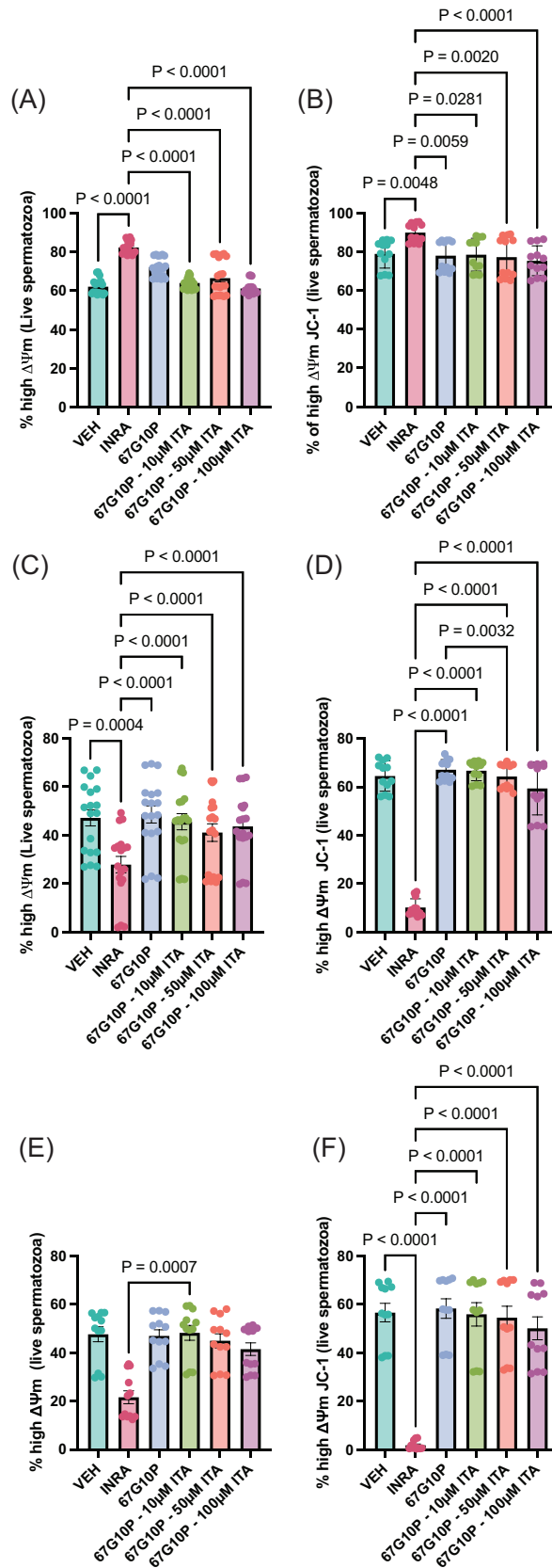


FIGURE 4 Continued

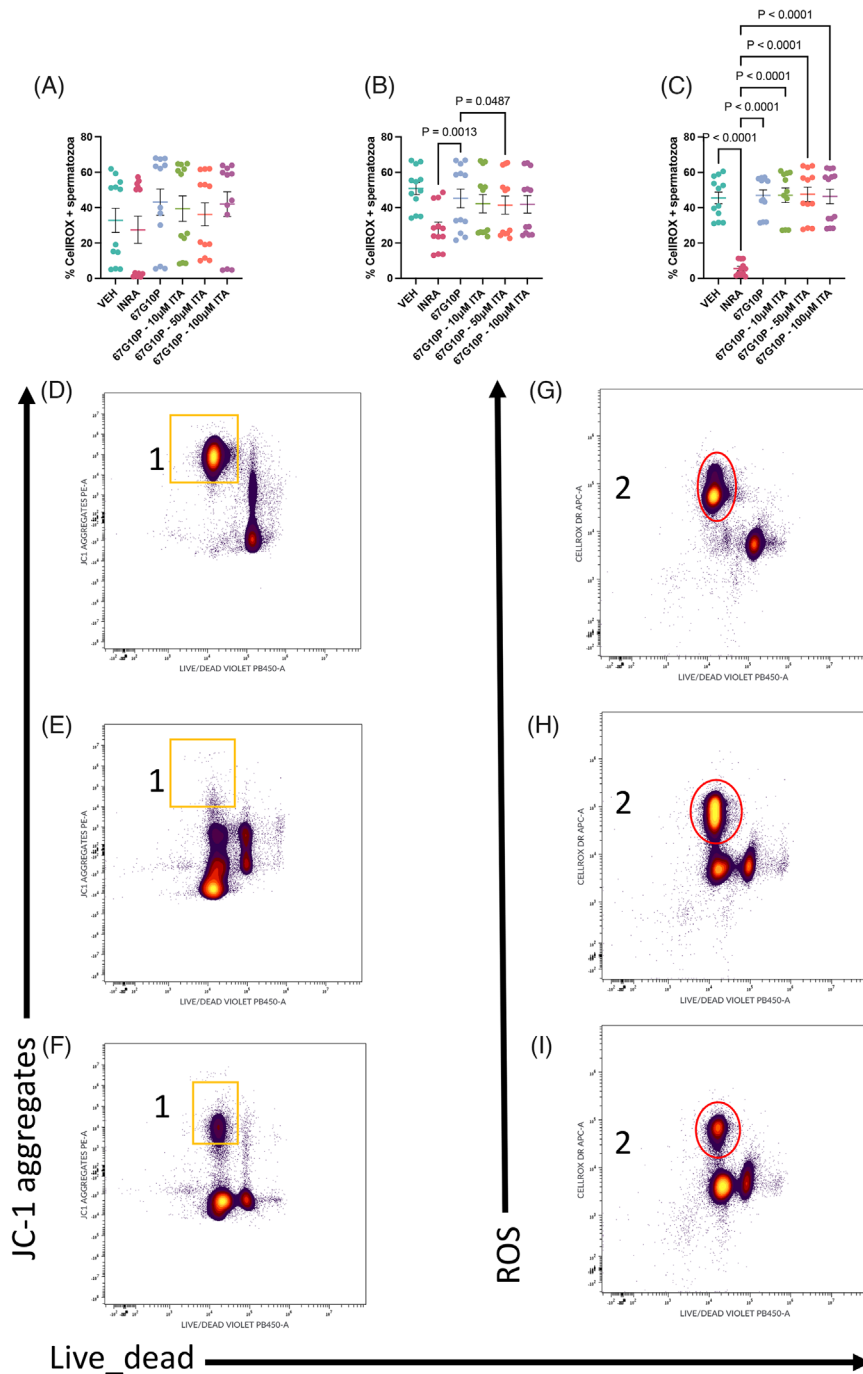


FIGURE 5 Production of reactive oxygen species (ROS) in stallion spermatozoa stored up to 96 h at 22°C. (A) Shortly after collection and processing ($t = 0$), (B) after 48 h of storage, and (C) after 96 h of storage. (D–G) Representative cytograms of the assay. (D) $\Delta\Psi_m$ measured in the population of live spermatozoa (1), live and dead spermatozoa are identified using a fixable Live/Dead violet probe, in this combination spectral overlap is negligible. In (G), the population of spermatozoa producing significant amounts of ROS is identified mainly in live spermatozoa, population (2), likely reflecting mitochondrial activity and production of $O_2^{\cdot-}$ as a subproduct of intense OXPHOS. However, as can be seen in (E) and (H), and to a lesser extent in (F) and (I), production of ROS unrelated to intense OXPHOS may be present. (E) Stallion spermatozoa with low $\Delta\Psi_m$, but which are producing significant amounts of ROS at the same time as seen in (H) (population (2)), these likely represent non-physiological production of ROS. Data are expressed as means \pm SEM and derived from three independent ejaculates from four different stallions ($n = 12$).

1 channels are opened,^{42,43} this opening seems to release “find me” signals, such as the nucleotides ATP and UTP, constituting a very early stage of apoptosis. Opening of these channels allows YoPro-1^{29,44,45} to stain these early apoptotic spermatozoa. Recent research has also revealed that YoPro-1⁺ spermatozoa are also those burdened with higher DNA fragmentation.⁴⁶ Interestingly, YoPro-1⁺ spermatozoa are characterized by low ATP content.⁴¹ In relation to these findings, metabolic mapping revealed that spermatozoa incubated in 67 mM glucose–10 mM pyruvate not only had lower percentages of YoPro-1⁺ staining, but also contained higher amounts of ATP than spermatozoa incubated in a media with only 67 mM glucose.

Mitochondrial membrane potential at the beginning of storage ($t = 0$) was higher in the control commercial INRA96, which dropped significantly after 48 and 96 h of storage. Interestingly, changes were more evident when the $\Delta\Psi_m$ was measured using JC-1, than when TMRM was used. Mitochondrial mass followed the same trend, being higher at the beginning of the storage in the control commercial extender, and dropping dramatically thereafter. Aliquots of stallion spermatozoa stored in the 67 mM glucose–10 mM pyruvate-based extenders, maintained mitochondrial mass over the entire storage period. It should be noted that the UMAP analysis revealed that mitochondrial mass and $\Delta\Psi_m$ were not equivalent, an

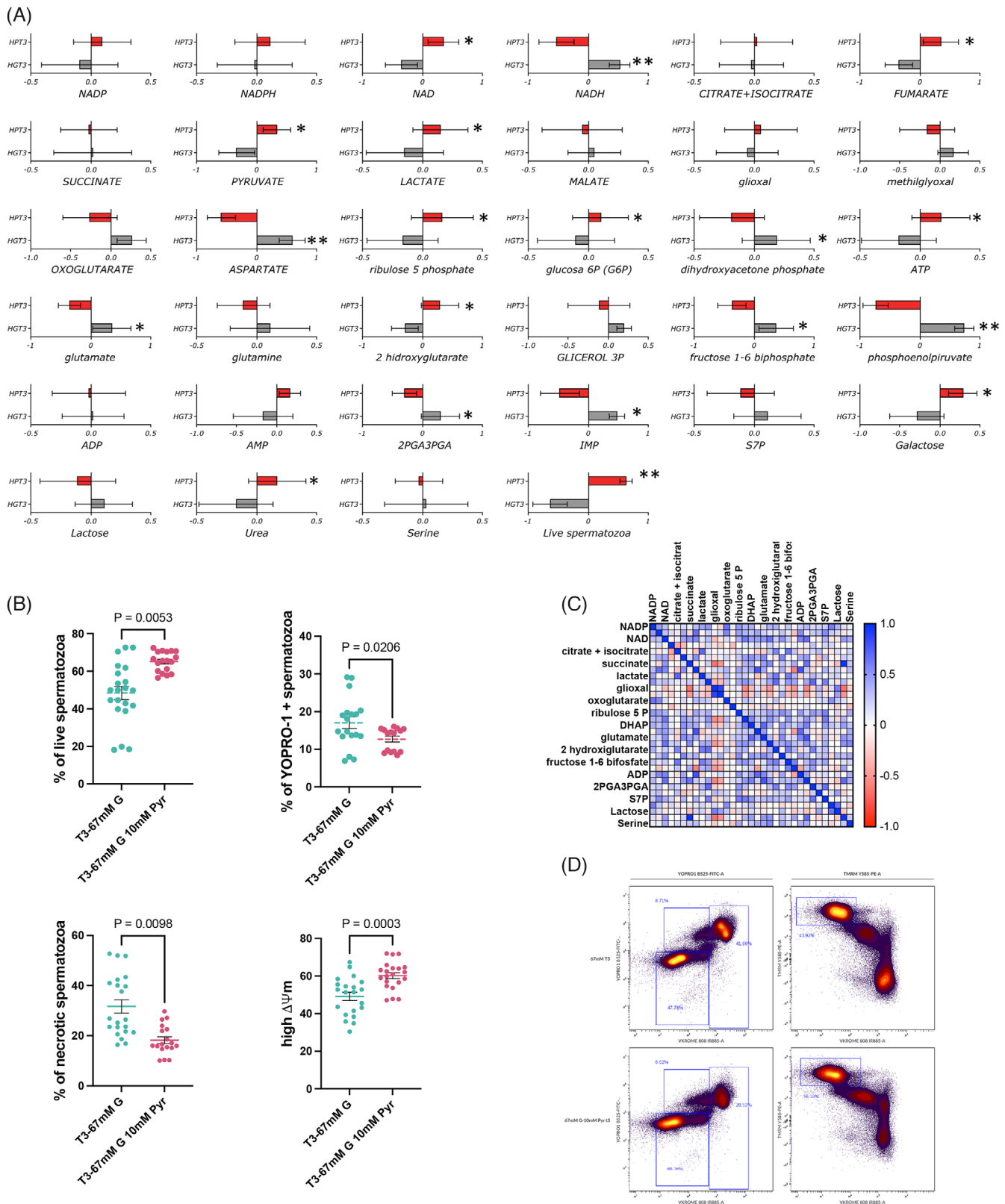


FIGURE 6 HPLC/MS/MS metabolic analysis of stallion spermatozoa incubated for 3 h at 37°C in two different media, Tyrode's modified 67 mM glucose and Tyrode's modified 67 mM glucose–10 mM pyruvate. (A) Changes in the relative content of selected metabolites of aliquots of the same stallion ejaculate incubated up to 3 h at 37°C in 67 mM modified Tyrode's (HGT3) or in 67 mM glucose–10 mM pyruvate-modified Tyrode's (HPT3). (B) Changes in the percentages of live, YoPro-1 positive, necrotic, and mitochondrial membrane potential. (C) Pearson correlations among the selected metabolites. (D) Representative cytograms after concatenation of the replicates of the flow cytometry assays. Data are expressed as means ± SEM and derived from three independent ejaculates from four different stallions (n = 12). *p < 0.05; **p < 0.01.

aspect to be considered when probes for mitochondrial analysis are chosen.

Production of ROS was investigated using CellROX Deep Red. It has been established that because of the the intense OXPHOS occurring in the mitochondria of stallion spermatozoa, the production of $O_2^{\cdot-}$ is significant in this species, a fact that was also evidenced in our study. However, interpretation of this phenomenon demands caution. This was especially evident during the simultaneous analysis of $\Delta\Psi_m$ and $O_2^{\cdot-}$, and better shown through UMAP analysis, in which sources of ROS associated with dysfunctional mitochondria were clearly identified; a phenomenon that was especially present when the control commercial extender was used and yet was lower in the spermatozoa stored in all the 67 mM glucose–10 mM pyruvate-based media. Similar findings have recently been reported by our laboratory,¹² when substantial production of ROS was observed in a commercial extender, but not in a low glucose–high pyruvate media.

Metabolic profiling was conducted to shed light on the mechanisms behind the improved functionality of the spermatozoa incubated in the pyruvate-based media, focusing on the effect of 10 mM pyruvate in a high-glucose media, 67 mM, a concentration widely used in commercial extenders, such as INRA96. Metabolomic analyses indicated that the improvement seen in the 67 mM glucose–10 mM pyruvate-based media was probably because of the the conversion of pyruvate to lactate, with the concomitant production of NAD^+ and increased glycolysis and the tricarboxylic acid cycle (TCA) efficiency.⁴⁷ NAD^+ serves as a cofactor for enzymes involved in glycolysis (glyceraldehyde phosphate dehydrogenase, oxidative decarboxylation of pyruvate to acetyl-CoA, e.g., pyruvate dehydrogenase), fatty acid β -oxidation (3-hydroxy acyl-CoA dehydrogenase), and tricarboxylic acid cycle (α -ketoglutarate, isocitrate, and malate dehydrogenases).⁴⁷ An improvement in glycolysis efficiency is supported by our finding of reduced phosphoenolpyruvate in the high-pyruvate media, and improvements in the TCA cycle supported by the increase in the relative amounts of malate and fumarate. Pyruvate also improved mitochondrial function, an effect that may be related to the role of NAD^+ as a cofactor of sirtuins and poly (ADP-ribose) polymerases (PARPs), either with potential roles as mitochondrial and metabolism regulators and pro-survival factors in spermatozoa.^{48,49} NAD^+ may be directly incorporated into the mitochondria,^{50–53} which is important in order to sustain the TCA cycle, generating metabolites to feed the electron transport chain (ETC) to produce ATP, and may also have important functions in the regulation of cell survival.⁵⁴ Additionally, recent research shows that lactate may activate and improve mitochondrial function by mechanisms independent of its metabolism.⁵⁵ Moreover, the stallion spermatozoa possesses a mitochondrial LDH isoform that may convert intramitochondrial lactate into pyruvate to be further metabolized in the TCA cycle.⁵⁶ In our study, addition of itaconate had no clear impact on sperm functionality, with respect to the 67 mM glucose–10 mM pyruvate medium, although some improvements were seen in sperm velocities and percentages of linear motile spermatozoa, which warrant further research. It is noteworthy that the best motility after 96 h of storage was seen in aliquots stored in the 67 mM glucose–10 mM pyruvate media supplemented with 10 μ M itaconate.

This effect was not as evident as seen in recent findings in pig spermatozoa in which the addition of itaconate improved sperm motility,²⁴ a species difference that may be related to the different metabolic strategies of the spermatozoa⁵⁷ and the varying composition of the media used in the studies. The study in pigs used 40 mM glucose. While stallion spermatozoa are highly dependent on OXPHOS for the generation of ATP, porcine spermatozoa seem to have a different metabolic strategy in which OXPHOS is present, but glycolysis predominates.^{57,58}

In summary, we show that stallion spermatozoa can be stored for up to 96 h at 22°C in a 67 mM glucose–10 mM pyruvate-based media. Aliquots stored in pyruvate-based media maintained a 35% motility after 96 h of storage at 22°C, which is considered the minimum acceptable motility for commercialization, without the need for cooling currently used. These pyruvate-based media maintained sperm quality, understood as sperm viability, mitochondrial membrane potential, motility, and kinematics. The improvements observed are related to the modifications in sperm metabolism, improving sperm survival. Our findings support the hypothesis that the use of more physiological extenders can improve semen storage and could be particularly useful for the distribution of commercial semen. The results warrant further follow-up research on the metabolism of the spermatozoa impacting current sperm technologies, as is also demonstrated in recent reports on the mechanism of sperm capacitation in horses.^{59,60}

AUTHOR CONTRIBUTIONS

Laura Becerro Rey conducted the experiments. Francisco E Martín Cano designed the study and conducted the experiments. Cristina Ortega Ferrusola and Heriberto Rodríguez-Martínez critically reviewed the manuscript. Gemma Gaitskell-Phillips performed the experiments and writing and editing (native English speaker). Eva da Silva-Álvarez and Antonio Silva-Álvarez performed experiments. María Cruz Gil obtained funding and critically reviewed experiments and manuscript. Fernando J. Peña obtained funding, designed, and administered the study, performed the formal data analysis, and drafted the manuscript. All authors read and approved the final version of the manuscript.

ACKNOWLEDGMENTS

The authors received financial support for this study from the Ministerio de Ciencia-European Fund for Regional Development (EFRD), Madrid, Spain (grant PID2021-122351OB-I00), Junta de Extremadura-FEDER (IB 20008), and Research Council FORMAS (Project 2019-00288), Stockholm, Sweden. Laura Becerro-Rey holds a PhD grant from the Ministry of Science, Madrid, Spain (PRE2022-103090).

CONFLICT OF INTEREST STATEMENT

The authors declare they have no potential conflicts of interest.

DATA AVAILABILITY STATEMENT

The data that support the findings of this study are available upon reasonable request from the corresponding author.

ORCID

Fernando J. Peña  <https://orcid.org/0000-0002-1311-2947>

REFERENCES

- Clulow J, Gibb Z. Liquid storage of stallion spermatozoa—Past, present and future. *Anim Reprod Sci.* 2022;247:107088. [10.1016/j.anireprosci.2022.107088](https://doi.org/10.1016/j.anireprosci.2022.107088)
- Gibb Z, Aitken RJ. Recent developments in stallion semen preservation. *J Equine Vet Sci.* 2016;43:S29-S36.
- Varner DD, Blanchard TL, Love CL, Garcia MC, Kenney RM. Effects of semen fractionation and dilution ratio on equine spermatozoal motility parameters. *Theriogenology.* 1987;28(5):709-723. [10.1016/0093-691x\(87\)90288-3](https://doi.org/10.1016/0093-691x(87)90288-3)
- Batellier F, Vidament M, Fauquant J, et al. Advances in cooled semen technology. *Anim Reprod Sci.* 2001;68(3-4):181-190. [10.1016/s0378-4320\(01\)00155-5](https://doi.org/10.1016/s0378-4320(01)00155-5)
- Ijaz A, Ducharme R. Effect of various extenders and taurine on survival of stallion sperm cooled to 5°C. *Theriogenology.* 1995;44(7):1039-1050. [10.1016/0093-691x\(95\)00290-o](https://doi.org/10.1016/0093-691x(95)00290-o)
- Eterpi M, Magistrini M, Couty I, et al. INRA96 supplemented with phospholipids liposomes, a promising approach for stallion sperm chilling. *J Equine Vet Sci.* 2022;108:103801. [10.1016/j.jevs.2021.103801](https://doi.org/10.1016/j.jevs.2021.103801)
- Batellier F, Gerard N, Courtens JL, Palmer E, Magistrini M. Preservation of stallion sperm quality by native phosphocaseinate: a direct or indirect effect? *J Reprod Fertil Suppl.* 2000(56):69-77.
- Pena FJ, Ortiz-Rodriguez JM, Gaitskell-Phillips GL, Gil MC, Ortega-Ferrusola C, Martin-Cano FE. An integrated overview on the regulation of sperm metabolism (glycolysis-Krebs cycle-oxidative phosphorylation). *Anim Reprod Sci.* 2022;246:106805. [10.1016/j.anireprosci.2021.106805](https://doi.org/10.1016/j.anireprosci.2021.106805)
- Ortega Ferrusola C, Gonzalez Fernandez L, Salazar Sandoval C, et al. Inhibition of the mitochondrial permeability transition pore reduces “apoptosis like” changes during cryopreservation of stallion spermatozoa. *Theriogenology.* 2010;74(3):458-465. [10.1016/j.theriogenology.2010.02.029](https://doi.org/10.1016/j.theriogenology.2010.02.029)
- Gibb Z, Lambourne SR, Aitken RJ. The paradoxical relationship between stallion fertility and oxidative stress. *Biol Reprod.* 2014;91(3):77. [10.1095/biolreprod.114.118539](https://doi.org/10.1095/biolreprod.114.118539)
- Darr CR, Varner DD, Teague S, Cortopassi GA, Datta S, Meyers SA. Lactate and pyruvate are major sources of energy for stallion sperm with dose effects on mitochondrial function, motility, and ROS production. *Biol Reprod.* 2016;95(2):34. [10.1095/biolreprod.116.140707](https://doi.org/10.1095/biolreprod.116.140707)
- Ortiz-Rodriguez JM, Martin-Cano FE, Gaitskell-Phillips GL, et al. Low glucose and high pyruvate reduce the production of 2-oxoaldehydes, improving mitochondrial efficiency, redox regulation, and stallion sperm function. *Biol Reprod.* 2021;105(2):519-532. [10.1093/biolre/iob073](https://doi.org/10.1093/biolre/iob073)
- Martin-Cano FE, Gaitskell-Phillips G, da Silva-Alvarez E, et al. The concentration of glucose in the media influences the susceptibility of stallion spermatozoa to ferroptosis. *Reproduction.* 2023;REP-23-0067. [10.1530/REP-23-0067](https://doi.org/10.1530/REP-23-0067)
- Luengo A, Li Z, Gui DY, et al. Increased demand for NAD⁺ relative to ATP drives aerobic glycolysis. *Mol Cell.* 2021;81(4):691-707. [10.1016/j.molcel.2020.12.012](https://doi.org/10.1016/j.molcel.2020.12.012). e6.
- Warburg O. On respiratory impairment in cancer cells. *Science.* 1956;124(3215):269-270.
- Hidalgo DM, Romarowski A, Gervasi MG, et al. Capacitation increases glucose consumption in murine sperm. *Mol Reprod Dev.* 2020;87(10):1037-1047. [10.1002/mrd.23421](https://doi.org/10.1002/mrd.23421)
- Numata S, McDermott JP, Sanchez G, Mitra A, Blanco G. The sodium-glucose cotransporter isoform 1 (SGLT-1) is important for sperm energetics, motility, and fertility. *Biol Reprod.* 2022;106(6):1206-1217. [10.1093/biolre/ioc052](https://doi.org/10.1093/biolre/ioc052)
- Portela JM, Tavares RS, Mota PC, Ramalho-Santos J, Amaral S. High glucose concentrations per se do not adversely affect human sperm function in vitro. *Reproduction.* 2015;150(1):77-84. [10.1530/REP-15-0100](https://doi.org/10.1530/REP-15-0100)
- Mannowetz N, Wandernoth PM, Wennemuth G. Glucose is a pH-dependent motor for sperm beat frequency during early activation. *PLoS One.* 2012;7(7):e41030. [10.1371/journal.pone.0041030](https://doi.org/10.1371/journal.pone.0041030)
- Williams AC, Ford WC. The role of glucose in supporting motility and capacitation in human spermatozoa. *J Androl.* 2001;22(4):680-695.
- Amaral A, Paiva C, Baptista M, Sousa AP, Ramalho-Santos J. Exogenous glucose improves long-standing human sperm motility, viability, and mitochondrial function. *Fertil Steril.* 2011;96(4):848-850. [10.1016/j.fertnstert.2011.07.1091](https://doi.org/10.1016/j.fertnstert.2011.07.1091)
- Hereng TH, Elgstoen KB, Cederkvist FH, et al. Exogenous pyruvate accelerates glycolysis and promotes capacitation in human spermatozoa. *Hum Reprod.* 2011;26(12):3249-3263. [10.1093/humrep/der317](https://doi.org/10.1093/humrep/der317)
- Chen F, Dowerg B, Cordes T. The yin and yang of itaconate metabolism and its impact on the tumor microenvironment. *Curr Opin Biotechnol.* 2023;84:102996. [10.1016/j.copbio.2023.102996](https://doi.org/10.1016/j.copbio.2023.102996)
- Zhu Z, Umehara T, Tsujita N, et al. Itaconate regulates the glycolysis/pentose phosphate pathway transition to maintain boar sperm linear motility by regulating redox homeostasis. *Free Radic Biol Med.* 2020;159:44-53. [10.1016/j.freeradbiomed.2020.07.008](https://doi.org/10.1016/j.freeradbiomed.2020.07.008)
- Morrell JM, Garcia BM, Pena FJ, Johannisson A. Processing stored stallion semen doses by single layer centrifugation. *Theriogenology.* 2011;76(8):1424-1432. [10.1016/j.theriogenology.2011.06.011](https://doi.org/10.1016/j.theriogenology.2011.06.011)
- Balao da Silva CM, Ortega Ferrusola C, Gallardo Bolanos JM, et al. Effect of overnight staining on the quality of flow cytometric sorted stallion sperm: comparison with traditional protocols. *Reprod Domest Anim.* 2014;49(6):1021-1027. [10.1111/rda.12431](https://doi.org/10.1111/rda.12431)
- Batellier F, Duchamp G, Vidament M, Arnaud G, Palmer E, Magistrini M. Delayed insemination is successful with a new extender for storing fresh equine semen at 15°C under aerobic conditions. *Theriogenology.* 1998;50(2):229-236. [10.1016/s0093-691x\(98\)00130-7](https://doi.org/10.1016/s0093-691x(98)00130-7)
- Ortega-Ferrusola C, Macias Garcia B, Suarez Rama V, et al. Identification of sperm subpopulations in stallion ejaculates: changes after cryopreservation and comparison with traditional statistics. *Reprod Domest Anim.* 2009;44(3):419-423. [10.1111/j.1439-0531.2008.01097.x](https://doi.org/10.1111/j.1439-0531.2008.01097.x)
- Gallardo Bolanos JM, Balao da Silva CM, Martin Munoz P, et al. Phosphorylated AKT preserves stallion sperm viability and motility by inhibiting caspases 3 and 7. *Reproduction.* 2014;148(2):221-235. [10.1530/REP-13-0191](https://doi.org/10.1530/REP-13-0191)
- Martin Munoz P, Ortega Ferrusola C, Vizuet G, Plaza Davila M, Rodriguez Martinez H, Pena FJ. Depletion of intracellular thiols and increased production of 4-hydroxynonenal that occur during cryopreservation of stallion spermatozoa lead to caspase activation, loss of motility, and cell death. *Biol Reprod.* 2015;93(6):143. [10.1095/biolreprod.115.132878](https://doi.org/10.1095/biolreprod.115.132878)
- Ortega-Ferrusola C, Anel-Lopez L, Martin-Munoz P, et al. Computational flow cytometry reveals that cryopreservation induces spermpptosis but subpopulations of spermatozoa may experience capacitation-like changes. *Reproduction.* 2017;153(3):293-304. [10.1530/REP-16-0539](https://doi.org/10.1530/REP-16-0539)
- Ahl PJ, Hopkins RA, Xiang WW, et al. Met-Flow, a strategy for single-cell metabolic analysis highlights dynamic changes in immune subpopulations. *Commun Biol.* 2020;3(1):305. [10.1038/s42003-020-1027-9](https://doi.org/10.1038/s42003-020-1027-9)
- Van Gassen S, Callebaut B, Van Helden MJ, et al. FlowSOM: using self-organizing maps for visualization and interpretation of cytometry data. *Cytometry A.* 2015;87(7):636-645. [10.1002/cyto.a.22625](https://doi.org/10.1002/cyto.a.22625)
- Stolarek I, Samelak-Czajka A, Figlerowicz M, Jackowiak P. Dimensionality reduction by UMAP for visualizing and aiding in classification of imaging flow cytometry data. *iScience.* 2022;25(10):105142. [10.1016/j.isci.2022.105142](https://doi.org/10.1016/j.isci.2022.105142)

35. Ujas TA, Obregon-Perko V, Stowe AM. A guide on analyzing flow cytometry data using clustering methods and nonlinear dimensionality reduction (tSNE or UMAP). *Methods Mol Biol.* 2023;2616:231-249. [10.1007/978-1-0716-2926-0_18](https://doi.org/10.1007/978-1-0716-2926-0_18)
36. Gaitskill-Phillips G, Martin-Cano FE, Ortiz-Rodriguez JM, et al. In stallion spermatozoa, superoxide dismutase (Cu-Zn) (SOD1) and the aldo-keto-reductase family 1 member b (AKR1B1) are the proteins most significantly reduced by cryopreservation. *J Proteome Res.* 2021;20(5):2435-2446. [10.1021/acs.jproteome.0c00932](https://doi.org/10.1021/acs.jproteome.0c00932)
37. Gaitskill-Phillips G, Martin-Cano FE, da Silva-Alvarez E, et al. Phosphoproteomics for the identification of new mechanisms of cryodamage: the role of SPATA18 in the control of stallion sperm function. *Biol Reprod.* 2023;108(2):324-337. [10.1093/biolre/iaoc211](https://doi.org/10.1093/biolre/iaoc211)
38. Pena FJ. Expanding the use of flow cytometry in semen analysis: the rise of flow spermometry. *Cytometry A.* 2023;103(6):465-469. [10.1002/cyto.a.24736](https://doi.org/10.1002/cyto.a.24736)
39. Hirata Y, Cai R, Volchuk A, et al. Lipid peroxidation increases membrane tension, Piezo1 gating, and cation permeability to execute ferroptosis. *Curr Biol.* 2023;33(7):1282-1294. [10.1016/j.cub.2023.02.060](https://doi.org/10.1016/j.cub.2023.02.060)
40. Van der Paal J, Neyts EC, Verlact CCW, Bogaerts A. Effect of lipid peroxidation on membrane permeability of cancer and normal cells subjected to oxidative stress. *Chem Sci.* 2016;7(1):489-498. [10.1039/c5sc02311d](https://doi.org/10.1039/c5sc02311d)
41. Balao da Silva CM, Ortega Ferrusola C, Morillo Rodriguez A, et al. Sex sorting increases the permeability of the membrane of stallion spermatozoa. *Anim Reprod Sci.* 2013;138(3-4):241-251. [10.1016/j.anireprosci.2013.02.021](https://doi.org/10.1016/j.anireprosci.2013.02.021)
42. Torres JL, Palomino J, Moreno RD, De Los Reyes M. Pannexin channels increase propidium iodide permeability in frozen-thawed dog spermatozoa. *Reprod Fertil Dev.* 2017;29(11):2269-2276. [10.1071/RD16267](https://doi.org/10.1071/RD16267)
43. Medina CB, Mehrotra P, Arandjelovic S, et al. Metabolites released from apoptotic cells act as tissue messengers. *Nature.* 2020;580(7801):130-135. [10.1038/s41586-020-2121-3](https://doi.org/10.1038/s41586-020-2121-3)
44. Sandilos JK, Chiu YH, Chekeni FB, et al. Pannexin 1, an ATP release channel, is activated by caspase cleavage of its pore-associated C-terminal autoinhibitory region. *J Biol Chem.* 2012;287(14):11303-11311. [10.1074/jbc.M111.323378](https://doi.org/10.1074/jbc.M111.323378)
45. Chekeni FB, Elliott MR, Sandilos JK, et al. Pannexin 1 channels mediate 'find-me' signal release and membrane permeability during apoptosis. *Nature.* 2010;467(7317):863-867. [10.1038/nature09413](https://doi.org/10.1038/nature09413)
46. Ribeiro SC, Sartorius G, Pletscher F, de Geyter M, Zhang H, de Geyter C. Isolation of spermatozoa with low levels of fragmented DNA with the use of flow cytometry and sorting. *Fertil Steril.* 2013;100(3):686-694. [10.1016/j.fertnstert.2013.05.030](https://doi.org/10.1016/j.fertnstert.2013.05.030)
47. Katsyuba E, Romani M, Hofer D, Auwerx J. NAD⁺ homeostasis in health and disease. *Nat Metab.* 2020;2(1):9-31. [10.1038/s42255-019-0161-5](https://doi.org/10.1038/s42255-019-0161-5)
48. Alam F, Syed H, Amjad S, Baig M, Khan TA, Rehman R. Interplay between oxidative stress, SIRT1, reproductive and metabolic functions. *Curr Res Physiol.* 2021;4:119-124. [10.1016/j.crphys.2021.03.002](https://doi.org/10.1016/j.crphys.2021.03.002)
49. Jha R, Agarwal A, Mahfouz R, et al. Determination of poly (ADP-ribose) polymerase (PARP) homologues in human ejaculated sperm and its correlation with sperm maturation. *Fertil Steril.* 2009;91(3):782-790. [10.1016/j.fertnstert.2007.12.079](https://doi.org/10.1016/j.fertnstert.2007.12.079)
50. Davila A, Liu L, Chellappa K, et al. Nicotinamide adenine dinucleotide is transported into mammalian mitochondria. *eLife.* 2018;7:e33246. [10.7554/eLife.33246](https://doi.org/10.7554/eLife.33246)
51. Pittelli M, Felici R, Pitozzi V, et al. Pharmacological effects of exogenous NAD on mitochondrial bioenergetics, DNA repair, and apoptosis. *Mol Pharmacol.* 2011;80(6):1136-1146. [10.1124/mol.111.073916](https://doi.org/10.1124/mol.111.073916)
52. Agrimi G, Brambilla L, Frascotti G, et al. Deletion or overexpression of mitochondrial NAD⁺ carriers in *Saccharomyces cerevisiae* alters cellular NAD and ATP contents and affects mitochondrial metabolism and the rate of glycolysis. *Appl Environ Microb.* 2011;77(7):2239-2246. [10.1128/AEM.01703-10](https://doi.org/10.1128/AEM.01703-10)
53. Luongo TS, Eller JM, Lu MJ, et al. SLC25A51 is a mammalian mitochondrial NAD⁺ transporter. *Nature.* 2020;588(7836):174-179. [10.1038/s41586-020-2741-7](https://doi.org/10.1038/s41586-020-2741-7)
54. Ying W. NAD⁺/NADH and NADP⁺/NADPH in cellular functions and cell death: regulation and biological consequences. *Antioxid Redox Signal.* 2008;10(2):179-206. [10.1089/ars.2007.1672](https://doi.org/10.1089/ars.2007.1672)
55. Cai X, Ng CC, Jones O, et al. Lactate activates the mitochondrial electron transport chain independent of its metabolism. *Mol Cell.* 2023;83(21):3904-3920.e7. [10.1101/2023.08.02.551712](https://doi.org/10.1101/2023.08.02.551712)
56. Swegen A, Curry BJ, Gibb Z, Lambourne SR, Smith ND, Aitken RJ. Investigation of the stallion sperm proteome by mass spectrometry. *Reproduction.* 2015;149(3):235-244. [10.1530/REP-14-0500](https://doi.org/10.1530/REP-14-0500)
57. Mateo-Otero Y, Madrid-Gambin F, Llanavera M, et al. Sperm physiology and in vitro fertilising ability rely on basal metabolic activity: insights from the pig model. *Commun Biol.* 2023;6(1):344. [10.1038/s42003-023-04715-3](https://doi.org/10.1038/s42003-023-04715-3)
58. Prieto OB, Algieri C, Spinaci M, Trombetti F, Nesci S, Bucci D. Cell bioenergetics and ATP production of boar spermatozoa. *Theriogenology.* 2023;210:162-168. [10.1016/j.theriogenology.2023.07.018](https://doi.org/10.1016/j.theriogenology.2023.07.018)
59. Ramirez-Agamez L, Hernandez-Aviles C, Ortiz I, Love CC, Varner DD, Hinrichs K. Lactate as the sole energy substrate induces spontaneous acrosome reaction in viable stallion spermatozoa. *Andrology.* 2023. [10.1111/andr.13479](https://doi.org/10.1111/andr.13479)
60. Hernandez-Aviles C, Ramirez-Agamez L, Varner DD, Love CC. Lactate-induced spontaneous acrosomal exocytosis as a method to study acrosome function in stallion sperm. *Theriogenology.* 2023;210:169-181. [10.1016/j.theriogenology.2023.07.024](https://doi.org/10.1016/j.theriogenology.2023.07.024)

SUPPORTING INFORMATION

Additional supporting information can be found online in the Supporting Information section at the end of this article.

How to cite this article: Becerro-Rey L, Martín-Cano FE, Ferrusola CO, et al. Aging of stallion spermatozoa stored in vitro is delayed at 22°C using a 67 mM glucose–10 mM pyruvate-based media. *Andrology.* 2023;1-16. <https://doi.org/10.1111/andr.13565>